Impacts of Salmon on Riparian Plant Diversity

Morgan D. Hocking* and John D. Reynolds

The study of natural gradients in nutrient subsidies between ecosystems allows for predictions of how changes in one system can affect biodiversity in another. We performed a large-scale empirical test of the role of Pacific salmon (*Oncorhynchus* spp.) in structuring riparian plant communities. A comparison of 50 watersheds in the remote Great Bear Rainforest of British Columbia's central coast in Canada shows that salmon influence nutrient loading to plants, shifting plant communities toward nutrient-rich species, which in turn decreases plant diversity. These effects are mediated by interactions between salmon density and the physical characteristics of watersheds. Predicting how salmon affect terrestrial ecosystems is central to conservation plans that aim to better integrate ecosystem values into resource management.

Declines in fish biomass through over-exploitation, habitat degradation, and climate change have important consequences for the structure and functioning of marine ecosystems (*1*). These changes to the marine environment can extend into coastal transition zones such as estuaries, mangroves, and streams, ultimately affecting the biodiversity and resilience of these communities (*2, 3*). However, marine species may play an even wider role in coastal ecology through nutrient subsidies to adjacent terrestrial ecosystems (*4, 5*). Tests are often restricted to small-scale observations or experiments and can overlook how physical and biological processes at local and regional scales may mediate the effects of subsidies on ecosystem structure and functioning (*6, 7*). Here, we tested the hypothesis that marine subsidies can affect terrestrial plant biodiversity across a large-scale gradient in anadromous fish biomass.

Throughout the North Pacific region, the largest cross-ecosystem movement of animals is the annual migration of wild salmon (*Oncorhynchus* spp.) from the ocean into freshwater streams and lakes, where they spawn and die. Adult salmon deliver marine nutrients to aquatic and terrestrial ecosystems and support the populations of many animal species (*8–10*). Declines in Pacific salmon populations throughout the 20th century have resulted in less salmon for fisheries and potential shifts in terrestrial ecosystem processes. Strong salmon populations provide benefits for bears (*Ursus* spp.) and other predators, and there are indications that salmon nutrients can affect riparian production (*8–10*). Nonetheless, uncertainty remains about the role of salmon in driving ecosystem-level structure and functioning. For example, salmon nutrient subsidies to freshwater systems are often counteracted by the physical disturbance of stream substrates associated with the digging of nests ("redds"), which can result in local nutrient export (*11, 12*). Also,

the productivity, size, and types of terrestrial habitats adjacent to salmon streams can mediate the effects of salmon subsidies, which vary markedly across their geographic range (*10, 13, 14*).

We used a large-scale survey from 50 watersheds on the central coast of British Columbia, Canada (*15*) (fig. S1 and table S1), to provide an empirical test of the relative influence of biotic and abiotic processes (i.e., salmon subsidy and physical habitat) in structuring plant nutrient uptake, community structure, and diversity. This region is relatively unaffected by industrial development and is part of the largest old-growth temperate rainforest in the world. Populations

of chum (*O. keta*), pink (*O. gorbuscha*), and coho (*O. kisutch*) salmon, and smaller numbers of sockeye (*O. nerka*) and Chinook (*O. tshawytscha*) salmon, spawn in hundreds of streams on remote islands and the adjacent mainland (*16*). From fall 2006 to fall 2009, we partnered with members of the Heiltsuk Nation to supplement existing federal programs that monitor salmon populations to derive an index of salmon spawning density (kilograms of salmon biomass per meter of spawning length) for each stream. We repeated all analyses with a 10-year mean (1997 to 2006) in a subset of streams (*n* = 25) where long-term salmon population data were available, and found very similar results (*15*) (tables S2 and S3). Intact habitats and low hunting pressure result in strong local populations of black bears (*U. americanus*), grizzly bears (*U. arctos horribilis*), wolves (*Canis lupus*), and other predators, which are important salmon consumers in this region (*17, 18*). They feed preferentially on energy-rich salmon parts and can transfer more than 50% of the salmon to the forest. Salmon carcasses can also provide pulsed increases in volatilized and in-stream nutrient concentrations, which can enter terrestrial systems via depositional and water-flow pathways. Although plant uptake of salmon nutrients has been demonstrated by testing for elevated heavy nitrogen ($\delta^{15}N$) (*19–22*), the key question is whether and how these subsidies alter riparian plant biodiversity.
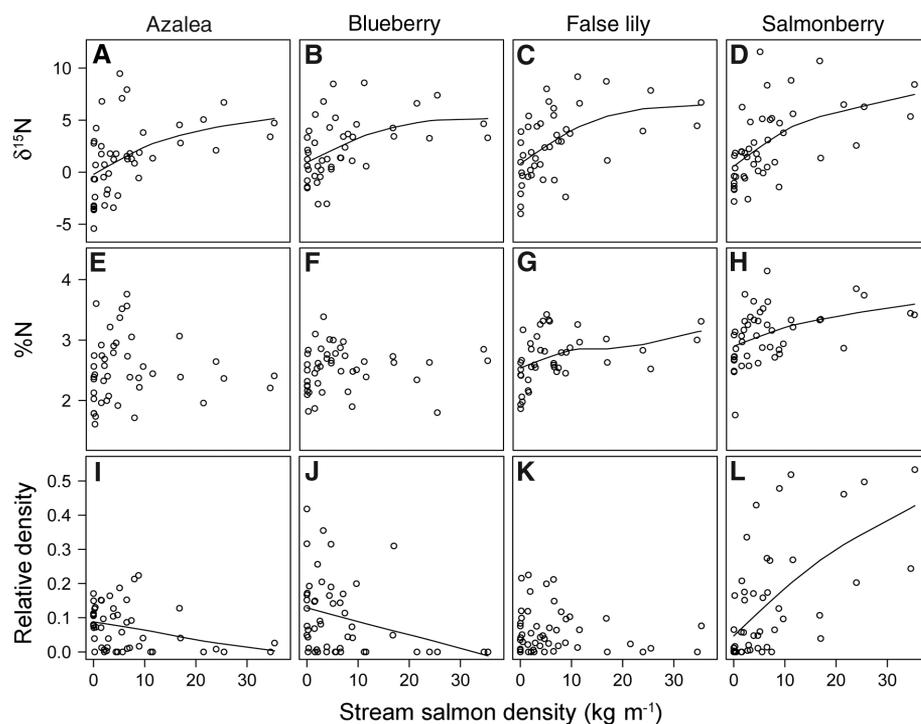

Fig. 1. Relationships between stream-level salmon spawning density (kg m^{-1}) and average foliar $\delta^{15}N$ (**A** to **D**), foliar %N (**E** to **H**), and plant abundance (cover/total shrub and herb cover) (**I** to **L**) in four dominant understory plant species—false azalea (*Menziesia ferruginea*), blueberry (*Vaccinium alaskaense* and *V. ovalifolium*), false lily-of-the-valley (*Maianthemum dilatatum*), and salmonberry (*Rubus spectabilis*)—sampled from 50 watersheds in coastal British Columbia. False azalea and blueberry indicate nutrient-poor soils, whereas false lily and, in particular, salmonberry are more competitive in nutrient-rich sites and are considered nitrophiles (*23*). Significant relationships are fitted using nonlinear LOESS smoothing.

Earth2Ocean Research Group, Department of Biological Sciences, Simon Fraser University, 8888 University Drive, Burnaby, British Columbia V5A 1S6, Canada.

*To whom correspondence should be addressed. E-mail: mhocking@sfu.ca

Table 1. The top-ranked model in each analysis. *N*, sample size; *k*, number of parameters; W_i, individual AIC model weights; R^2, coefficient of fitted versus observed values for each analysis. Parameter estimates and top model fits are shown in tables S10 to S13 and fig. S4.
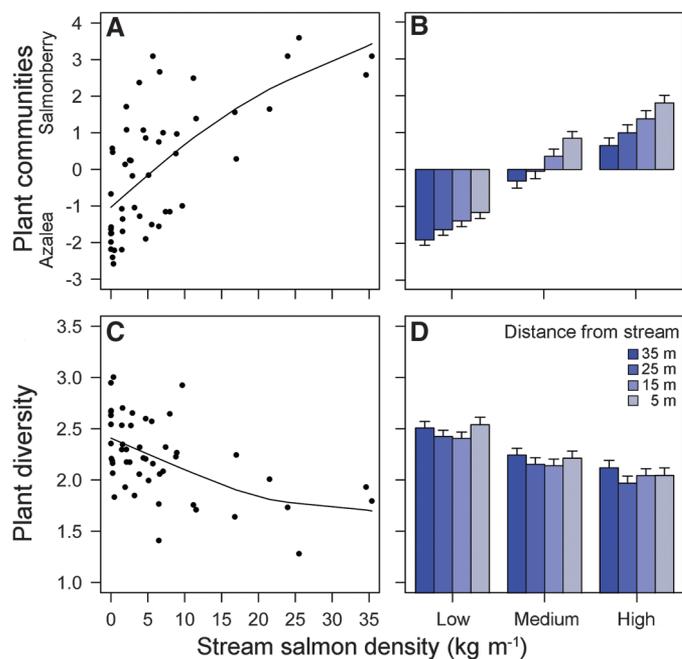
Analysis	Parameters in top-ranked model	N	k	W_i	R^2
1. Foliar δ^{15}N	Salmon density [log (x + 1)], canopy community, soil moisture index	906	21	0.99	0.66
	Foliar %N, plant species, foliar %N × plant species				
	Salmon density × plant species				
	Salmon density × foliar %N				
2. Foliar %N	Salmon density [log (x + 1)], canopy community, watershed size, stem density, site slope	906	20	0.92	0.50
	Plant species, salmon density × plant species				
	Salmon density × canopy community				
	Salmon density × site slope				
3. Plant communities	Salmon density, site slope, distance from stream	1192	13	0.60	0.81
	Canopy community				
	Salmon density × canopy community				
4. Plant diversity	Salmon density, canopy community, watershed size, stem density	1192	15	0.24	0.51
	Site slope, canopy cover, course woody debris cover, distance from stream				
	Salmon density × site slope				

Fig. 2. Relationships between stream-level salmon spawning density (kg m⁻¹) and understory plant community structure (PC1) (**A** and **B**) and plant diversity (D_{Mg}) (**C** and **D**) in 50 watersheds in coastal British Columbia. In (A) and (C), relationships are fitted using nonlinear LOESS smoothing; in (B) and (D), they are fitted by distance from the stream (5 to 35 m) split by evenly weighted categories (low, medium, high) of stream-level salmon spawning density (± SEM).

From June to mid-July 2007, we measured the percent cover of all forest plant species, including shrubs, herbs, ferns, mosses, liverworts, and understory trees (*n* = 104 species), within 1-m² plots (*n* = 1200) placed 5, 15, 25, and 35 m from the stream edge (6 transects per watershed × 50 watersheds). We also collected foliar samples for nutrient and stable isotope analyses from four dominant plant species (Fig. 1). Understory plant community structure was quantified into axes of variation via principal components analysis (PCA) (table S4). The first axis of understory plant community variation at the watershed scale (PC1 = 31.1%) was strongly correlated to an established nitrogen indicator classification system in coastal British Columbia (*23*) (fig. S2).

We used hierarchical linear mixed-effects (LME) modeling (*24, 25*) and model selection via the Akaike information criterion (AIC$_c$) to predict variation within and across watersheds in four dependent variables: (i) leaf δ^{15}N signatures, (ii) total leaf nitrogen (%N), (iii) understory plant community structure (PC1), and (iv) understory plant diversity (Margalef's D_{Mg}). First, on the basis of a priori hypotheses of up to 12 separate habitat variables, we derived a best-fit habitat-only model for each of the four dependent variables (*15*) (tables S5 to S8), informed by the long history of forest habitat analyses in British Columbia (*23, 26, 27*). For example, we assessed canopy community structure across spatial scales from individual plots to watersheds, including the prevalence of the nitrogen-fixing red alder (*Alnus rubra*), which can have a strong influence on local nutrient dynamics (*14*). The first axis of canopy community variation (Canopy PC1 = 36.1%) at the watershed scale described a shift from low-productivity forests dominated by western redcedar (*Thuja plicata*) to more productive forests dominated by red alder and Sitka spruce (*Picea sitchensis*). This axis is predicted by a broad climatic gradient and by watershed size (fig. S3), but only weakly by salmon spawning density (*15*).

In the second step of the analysis, for each dependent variable we compared the best-fit habitat-only models (hypothesis 1) with salmon-only models [log(salmon density in kg m⁻¹); hypothesis 2], salmon density + best-fit habitat models (hypothesis 3), and models containing salmon density, best-fit habitat, and a priori predictions of salmon density × habitat interactions (hypothesis 4) (*15*) (tables S7 and S9). This enabled a test of the hypothesis that salmon and habitat would interact to structure plant biodiversity.

All plant species showed increases in δ^{15}N across the watershed-level gradient in salmon spawning density (Fig. 1, A to D). The top foliar δ^{15}N model included strong effects of salmon (LME: t_{42} = 6.4, P < 0.0001), habitat, and salmon × habitat interactions, including interactions with total leaf nitrogen (Table 1 and table S10). This shows that increases in leaf δ^{15}N with salmon density are caused by both the δ^{15}N-enriched source of nitrogen from salmon (~12‰) and high-

er total nitrogen availability (e.g., through increased nitrification) (*22, 28*). Streams with high salmon densities also had plants with high total leaf nitrogen (LME: t_{42} = 3.0, P = 0.005), driven by strong relationships in two nutrient-rich indicator species, false lily-of-the-valley and salmonberry (Fig. 1, E to H, Table 1, and table S11). We observed positive relationships between leaf δ^{15}N and %N, which can be caused by salmon subsidies and gradients in soil nutrients, site productivity, and plant dependence on mycorrhizal fungi for nitrogen uptake (*29–31*). Changes in the slope of leaf δ^{15}N by %N across plant species and the gradient in salmon density imply that although many coastal watersheds may be nitrogen-limited, nitrogen can be saturating when salmon resource subsidies are high.

Salmonberry was the only sampled species that increased in abundance across the gradient in

Fig. 3. Productivity and habitat mediate the effect of salmon on plant biodiversity. (**A**) Plants growing in less productive sites with lower leaf %N show greater increases in foliar δ^{15}N with salmon density than plants growing in more productive sites with higher %N. (**B** and **C**) Watersheds dominated by red alder (*Alnus rubra*) have saturated leaf %N and nutrient-rich plant communities relative to watersheds with canopies dominated by western redcedar (*Thuja plicata*), which show large shifts in nutrient use and community structure across stream salmon spawning density. (**D**) The streamside slope mediates the decrease in plant diversity across the gradient in salmon density. Predictions are based on top model parameter estimates (tables S10 to S13).
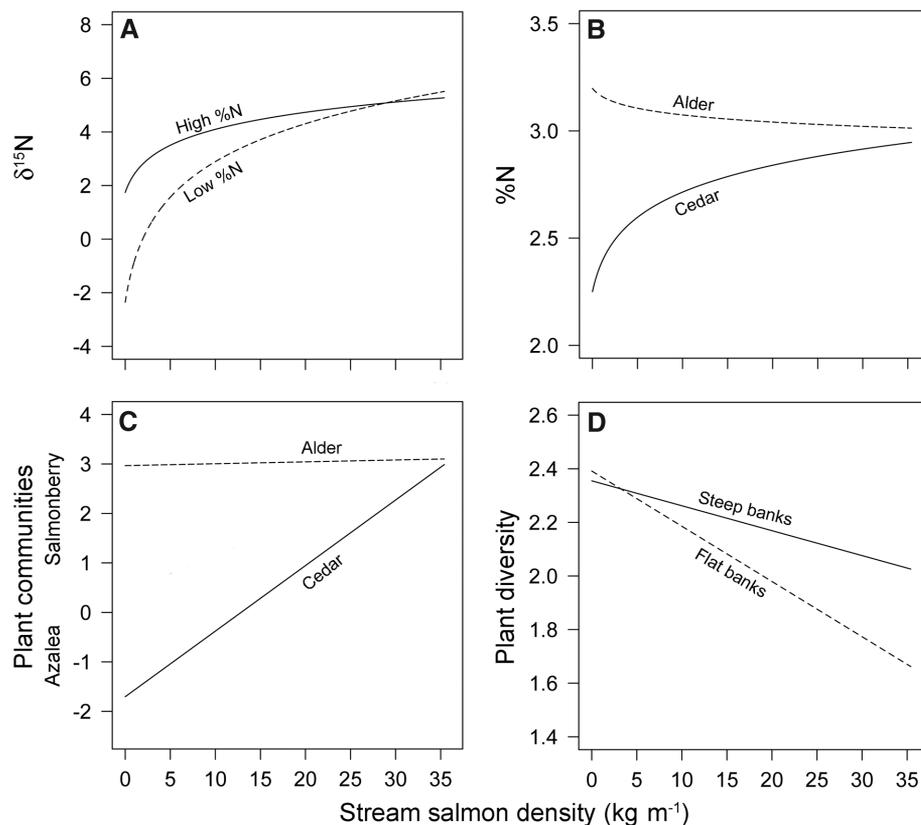
Table 2. The weight of evidence supporting each hypothesis in all four analyses. Shown are the AIC weights (W_i) when the best model from within each hypothesis is competed against the other three hypotheses. In parentheses are the total numbers of models considered within each hypothesis.

Analysis	1. Habitat	2. Salmon density	3. Habitat and salmon density	4. Habitat, salmon density, and interactions
1. Foliar δ^{15}N	0.0% (7)	0.0% (4)	0.4% (5)	99.6% (4)
2. Foliar %N	0.03% (5)	0.05% (4)	1.3% (4)	98.6% (4)
3. Plant communities	0.01% (9)	0.0% (4)	16.7% (3)	83.2% (6)
4. Plant diversity	1.4% (6)	0.2% (4)	41.2% (4)	57.2% (6)

salmon density (Fig. 1, I to L). Salmonberry also had the highest average foliar δ^{15}N and %N, the strongest relationships of δ^{15}N and %N with salmon density, and the weakest positive slope of δ^{15}N with foliar %N (table S10). Salmonberry is a strong nitrophile and has arbuscular mycorrhizal associations that facilitate plant access to nutrients, especially phosphorus (*23, 31*). In contrast, false azalea and blueberry decreased in abundance across the gradient in salmon density (Fig. 1, I and J). These species have ericoid mycorrhizal associations that facilitate organic nitrogen uptake in nutrient-limited conditions, and are likely restricted to nutrient-poor microsites such as decaying woody debris in highly productive watersheds.

Patterns of abundance and nutrient uptake in individual species translate to shifts in overall plant biodiversity (Fig. 2). There was a shift in dominance from plant species typical of nutrient-poor habitats in watersheds with low salmon density toward plants typical of nutrient-rich habitats in watersheds with high salmon density (LME: $t_{46} = 5.0$, $P < 0.0001$). This shift resulted in a decrease

in plant diversity (LME: $t_{46} = -3.4$, $P = 0.001$). The top models predicting understory community structure and diversity had strong effects of salmon density, habitat, and salmon density × habitat interactions (Table 1 and tables S12 and S13). Patterns of plant diversity show that plant communities in salmon-rich watersheds become dominated by a few species (*15*), in particular the nutrient-rich shrubs salmonberry and stink currant (*Ribes bracteosum*). Shifts in plant communities were observed with distance from the stream edge (to 35 m), although these effects were similar across the gradient in salmon density (Fig. 2, B and D).

The explicit incorporation of habitat variables that describe shifts in terrestrial ecosystem structure across multiple spatial scales enables predictions of how habitats may mediate the effects of salmon in terrestrial environments (*32*). Variation in physical habitats and background nitrogen levels within and across watersheds strongly influenced plant nitrogen uptake and community composition (Fig. 3 and fig. S5). In each analysis, the overwhelming weight of evidence supported either hypothesis 3 (salmon density + habitat) or

hypothesis 4 (salmon density + habitat + salmon density × habitat interactions) (Table 2). There was very low support (< 1%) for the hypotheses that only habitat or salmon density predict foliar δ^{15}N, %N, plant community structure, or diversity. The dominant habitat predictors almost always included the canopy community composition and site slope. Background %N was a key driver of foliar δ^{15}N. Interactions between these variables and salmon density show that salmon have lower effects in large watersheds dominated by red alder canopies, where high terrestrial productivity and nitrogen fixation likely overwhelm salmon inputs, and in sites with steep slopes, probably through decreased predator access to salmon and reduced retention of carcasses and nutrients (Fig. 3).

There has been a push toward management objectives that incorporate wider ecosystem values related to salmon (*33–36*). For example, as management strategies begin to incorporate the ecological importance of salmon when setting salmon population targets (*34*), it has become increasingly important to understand the links between salmon caught in fisheries and changes to

ecosystem structure. Our study shows that declines in salmon will have the largest ecological impacts on smaller and less productive streams. In contrast, large and shallow-sloped watersheds dominated by nitrogen-fixing red alders are predicted to be more resilient to salmon declines. These considerations enable predictions of impacts of anthropogenic stressors across ecosystem boundaries, which can then be incorporated into ecosystem-based management.

References and Notes

1. B. Worm et al., Science 314, 787 (2006).
2. J. B. C. Jackson et al., Science 293, 629 (2001).
3. H. K. Lotze et al., Science 312, 1806 (2006).
4. G. A. Polis, S. D. Hurd, Am. Nat. 147, 396 (1996).
5. D. A. Croll, J. L. Maron, J. A. Estes, E. M. Danner, G. V. Byrd, Science 307, 1959 (2005).
6. J. L. Maron et al., Ecol. Monogr. 76, 3 (2006).
7. L. B. Marczak, R. M. Thompson, J. S. Richardson, Ecology 88, 140 (2007).
8. S. M. Gende, R. T. Edwards, M. F. Willson, M. S. Wipfli, Bioscience 52, 917 (2002).
9. R. J. Naiman, R. E. Bilby, D. E. Schindler, J. M. Helfield, Ecosystems 5, 399 (2002).
10. D. J. Janetski, D. T. Chaloner, S. D. Tiegs, G. A. Lamberti, Oecologia 159, 583 (2009).
11. J. W. Moore, D. E. Schindler, Can. J. Fish. Aquat. Sci. 61, 1582 (2004).
12. J. W. Moore et al., Ecology 88, 1278 (2007).
13. S. D. Tiegs et al., Ecol. Appl. 18, 4 (2008).
14. J. M. Helfield, R. J. Naiman, Oecologia 133, 573 (2002).
15. See supporting material on Science Online.
16. M. H. H. Price, C. T. Darimont, N. F. Temple, S. M. MacDuffee, Can. J. Fish. Aquat. Sci. 65, 2712 (2008).
17. T. E. Reimchen, Can. J. Zool. 78, 448 (2000).
18. C. T. Darimont, P. C. Paquet, T. E. Reimchen, BMC Ecol. 8, 14 (2008).
19. R. E. Bilby, B. R. Fransen, P. A. Bisson, Can. J. Fish. Aquat. Sci. 53, 164 (1996).
20. K. K. Bartz, R. J. Naiman, Ecosystems 8, 529 (2005).
21. C. E. Wilkinson, M. D. Hocking, T. E. Reimchen, Oikos 108, 85 (2005).
22. M. D. Hocking, T. E. Reimchen, Oikos 118, 1307 (2009).
23. K. Klinka, V. J. Krajina, A. Ceska, A. M. Scagel, Indicator Plants of Coastal British Columbia (Univ. of British Columbia Press, Vancouver, 1989).
24. J. M. Diez, H. R. Pulliam, Ecology 88, 3144 (2007).
25. A. F. Zuur, E. N. Ieno, N. J. Walker, A. A. Saveliev, G. M. Smith, Mixed Effects Models and Extensions in Ecology with R (Springer Science+Business Media, New York, 2009).
26. P. A. Alaback, Ecology 63, 1932 (1982).
27. J. Pojar, K. Klinka, D. V. Meidinger, For. Ecol. Manage. 22, 119 (1987).
28. G. Pinay, T. O'Keefe, R. Edwards, R. J. Naiman, Ecosystems 6, 336 (2003).
29. E. A. Hobbie, J. E. Hobbie, Ecosystems 11, 815 (2008).
30. J. M. Craine et al., New Phytol. 183, 980 (2009).
31. J. M. Kranabetter, W. H. MacKenzie, Ecosystems 13, 108 (2010).
32. J. J. Verspoor, D. C. Braun, J. D. Reynolds, Ecosystems 13, 1020 (2010).
33. R. E. Bilby, B. R. Fransen, J. K. Walter, C. J. Cederholm, W. J. Scarlett, Fisheries 26, 6 (2001).
34. DFO (Fisheries and Oceans Canada, Vancouver, 2005).
35. C. T. Darimont et al., Conserv. Lett. 3, 379 (2010).
36. D. E. Schindler et al., Nature 465, 609 (2010).

CD40 Agonists Alter Tumor Stroma and Show Efficacy Against Pancreatic Carcinoma in Mice and Humans

Gregory L. Beatty,[1,2,6] Elena G. Chiorean,[3] Matthew P. Fishman,[1] Babak Saboury,[5] Ursina R. Teitelbaum,[2,6] Weijing Sun,[2,6] Richard D. Huhn,[4] Wenru Song,[4] Dongguang Li,[4] Leslie L. Sharp,[4] Drew A. Torigian,[2,5] Peter J. O'Dwyer,[2,6] Robert H. Vonderheide[1,2,6]*

Immunosuppressive tumor microenvironments can restrain antitumor immunity, particularly in pancreatic ductal adenocarcinoma (PDA). Because CD40 activation can reverse immune suppression and drive antitumor T cell responses, we tested the combination of an agonist CD40 antibody with gemcitabine chemotherapy in a small cohort of patients with surgically incurable PDA and observed tumor regressions in some patients. We reproduced this treatment effect in a genetically engineered mouse model of PDA and found unexpectedly that tumor regression required macrophages but not T cells or gemcitabine. CD40-activated macrophages rapidly infiltrated tumors, became tumoricidal, and facilitated the depletion of tumor stroma. Thus, cancer immune surveillance does not necessarily depend on therapy-induced T cells; rather, our findings demonstrate a CD40-dependent mechanism for targeting tumor stroma in the treatment of cancer.

Pancreatic ductal adenocarcinoma (PDA) remains an almost universally lethal disease; chemotherapy offers minimal benefit over best supportive care for patients who are not surgical candidates (1). We have previously demonstrated that leukocytes actively infiltrate the stromal compartment of PDA, even at the earliest stages of tumor development, and orchestrate an immune reaction that is immunosuppressive (2). In this study, we investigated the reversibility of this immune suppression, hy-

pothesizing initially that doing so would unleash tumor-specific cellular immunity to eliminate PDA. Activation of the tumor necrosis factor (TNF) receptor superfamily member CD40 has been shown to be a key regulatory step in the development of T cell–dependent antitumor immunity, which relies on CD40-mediated "licensing" of antigen-presenting cells (APCs) for tumor-specific T cell priming and activation (3–8).

On the basis of this premise, we investigated in both humans and mice whether systemic CD40

activation with an agonist CD40 monoclonal antibody (mAb) can circumvent tumor-induced immune suppression and invoke productive T cell–dependent antitumor immunity in PDA. We first evaluated the clinical impact of CD40 activation by performing a clinical trial of the fully human agonist CD40 mAb CP-870,893 (9) in combination with gemcitabine chemotherapy (2′-deoxy-2′,2′-difluorocytidine) for patients with chemotherapy-naïve, surgically incurable PDA (10). We tested CP-870,893 with gemcitabine because chemotherapy delivered before an agonist CD40 mAb can facilitate enhanced tumor antigen presentation by APCs (11–14). Twenty-one patients (90% with metastatic disease) received gemcitabine weekly on days 1, 8, and 15 with CP-870,893 administered on day 3 of each 28-day cycle (fig. S1). Treatment was well tolerated overall (fig. S2), and the most common side effect was mild-to-moderate cytokine release syndrome characterized by chills, fevers, rigors, and other symptoms on the day of CP-870,893

[1]Abramson Family Cancer Research Institute, University of Pennsylvania School of Medicine, 421 Curie Boulevard, Philadelphia, PA 19104, USA. [2]Abramson Cancer Center, University of Pennsylvania School of Medicine, Philadelphia, PA 19104, USA. [3]Division of Hematology/Oncology, Department of Medicine, Indiana University School of Medicine, Indianapolis, IN 46202, USA. [4]Pfizer Corporation, New London, CT 06320, USA. [5]Department of Radiology, Department of Medicine, University of Pennsylvania School of Medicine, Philadelphia, PA 19104, USA. [6]Division of Hematology-Oncology, Department of Medicine, University of Pennsylvania School of Medicine, Philadelphia, PA 19104, USA.

*To whom correspondence should be addressed. E-mail: rhv@exchange.upenn.edu